bioRxiv preprint doi: https://doi.org/10.1101/663088; this version posted June 6, 2019. The copyright holder for this preprint (which was not certified by peer review) is the author/funder, who has granted bioRxiv a license to display the preprint in perpetuity. It is made available under aCC-BY 4.0 International license.

Functional analyses of *STIM1* mutations reveal a common pathomechanism for tubular aggregate myopathy and Stormorken syndrome

Georges Arielle Peche[1,2,3,4], Coralie Spiegelhalter[1,2,3,4], Roberto Silva-Rojas[1,2,3,4], Jocelyn Laporte[1,2,3,4*], Johann Böhm[1,2,3,4*]

[1]Institut de Génétique et de Biologie Moléculaire et Cellulaire (IGBMC), 67404 Illkirch, France

[2]INSERM U1258, 67404 Illkirch, France

[3]CNRS, UMR7104, 67404 Illkirch, France

[4]Université de Strasbourg, 67404 Illkirch, France

*The authors contributed equally to this work

Correspondence: Johann Böhm, Jocelyn Laporte

IGBMC, 1 Rue Laurent Fries, 67404 Illkirch

johann@igbmc.fr / jocelyn@igbmc.fr

Tel: 0033 (0)3 88 65 34 12

bioRxiv preprint doi: https://doi.org/10.1101/663088; this version posted June 6, 2019. The copyright holder for this preprint (which was not certified by peer review) is the author/funder, who has granted bioRxiv a license to display the preprint in perpetuity. It is made available under aCC-BY 4.0 International license.

ABSTRACT

Tubular aggregate myopathy (TAM) is a progressive disorder essentially involving muscle weakness, cramps, and myalgia. TAM clinically overlaps with Stormorken syndrome (STRMK), associating TAM with miosis, thrombocytopenia, hyposplenism, ichthyosis, short stature, and dyslexia. TAM and Stormorken syndrome arise from gain-of-function mutations in *STIM1* or *ORAI1*, both encoding key regulators of Ca^{2+} homeostasis, and mutations in either gene results in excessive Ca^{2+} entry. The pathomechanistic similarities and differences of TAM and Stormorken syndrome are only partially understood. Here we provide functional *in cellulo* experiments demonstrating that STIM1 harboring the TAM D84G or the STRMK R304W mutation similarly cluster and exert a dominant effect on the wild-type protein. Both mutants recruit ORAI1 to the clusters, induce major nuclear import of the Ca^{2+}-dependent transcription factor NFAT, and trigger the formation of circular membrane stacks. In conclusion, the analyzed TAM and STRMK mutations have a comparable impact on STIM1 protein function and downstream effects of excessive Ca^{2+} entry, highlighting that TAM and Stormorken syndrome involve a common pathomechanism.

Keywords: STIM1, tubular aggregate myopathy, Stormorken syndrome, SOCE, calcium

bioRxiv preprint doi: https://doi.org/10.1101/663088; this version posted June 6, 2019. The copyright holder for this preprint (which was not certified by peer review) is the author/funder, who has granted bioRxiv a license to display the preprint in perpetuity. It is made available under aCC-BY 4.0 International license.

INTRODUCTION

Tubular aggregate myopathy (TAM) and Stormorken syndrome (STRMK) are spectra of the same disease affecting muscle, platelets, spleen, and skin (1, 2). The majority of the TAM patients primarily present with muscle weakness, cramps, and myalgia with a heterogeneous age of onset and disease severity (3-6). Additional features including thrombocytopenia, hyposplenism, miosis, ichthyosis, short stature, hypocalcemia, or dyslexia can be seen as well, and the occurrence of the totality of the multi-systemic signs constitutes the diagnosis of Stormorken syndrome (7-18).

Both TAM and Stormorken syndrome are characterized by the presence of densely packed membrane tubules in muscle fibers, and investigations on muscle sections by immunofluorescence have shown that these tubular aggregates contain various sarcoplasmic reticulum (SR) proteins, suggesting that they originate from the SR (4, 7, 15, 16, 19). The tubular aggregates are the histopathological hallmark of TAM and Stormorken syndrome, and were also described in hypokalemic periodic paralysis, myasthenic syndrome, malignant hyperthermia, inflammatory or ethyltoxic myopathy, and accumulate in normal muscle with age (20-25).

TAM and Stormorken syndrome are caused by heterozygous missense mutations in *STIM1* (4, 10-12) (OMIM #605921) or *ORAI1* (12) (OMIM #610277), both encoding key factors of store-operated Ca^{2+} entry (SOCE). SOCE is a major mechanism regulating Ca^{2+} homeostasis and thereby drives a multitude of Ca^{2+}-dependent cellular functions including muscle contraction. STIM1 has a single transmembrane domain and is primarily localized at the endoplasmic/sarcoplasmic reticulum with an N-terminal luminal part containing the Ca^{2+}-sensing EF hands, and a C-terminal cytosolic part containing coiled-coil domains (CC1-3). Upon Ca^{2+} store depletion, STIM1 undergoes a conformational change, clusters in vicinity to

bioRxiv preprint doi: https://doi.org/10.1101/663088; this version posted June 6, 2019. The copyright holder for this preprint (which was not certified by peer review) is the author/funder, who has granted bioRxiv a license to display the preprint in perpetuity. It is made available under aCC-BY 4.0 International license.

the plasma membrane, and recruits and activates the Ca^{2+} channel ORAI1 to trigger extracellular Ca^{2+} entry and reticular Ca^{2+} store refill (26-28). Functional experiments have shown that the *STIM1* and *ORAI1* mutations induce excessive extracellular Ca^{2+} entry despite replete reticular Ca^{2+} stores (4, 10-12, 15).

Fourteen different *STIM1* mutations have been described in patients with TAM and Stormorken syndrome, including 12 mutations in the luminal EF-hands, and two mutations in the cytosolic CC1 domain (3-14, 18). Patients with EF-hand mutations mainly manifest a muscle phenotype and only isolated multi-systemic features, while the most common R304W substitution in the cytosolic CC1 domain, found in thirteen unrelated families, was essentially described with the full clinical picture of Stormorken syndrome (7, 10-14).

The shared genetic causes of TAM and Stormorken syndrome, the consistent skeletal muscle histopathology, and the overlapping clinical presentation of affected individuals raises the possibility of a common sequence of events leading to either TAM or STRMK. In an attempt to elucidate and compare the cellular defects underlying both disorders, we performed a series of functional and comparative *in cellulo* experiments. We demonstrate that both the TAM D84G and the STRMK R304W mutation similarly impact on STIM1 migration and clustering at the plasma membrane, the interaction with ORAI1, the nuclear translocation of the Ca^{2+}-dependent transcription factor NFAT, and the formation of membrane stacks. We therefore conclude that TAM and Stormorken syndrome involve a common pathomechanism.

MATERIALS AND METHODS

Constructs

The human YFP-STIM1, mCherry-STIM1, ORAI1-eGFP, and eGFP-NFAT constructs were kind gifts from Nicolas Demaurex (University of Geneva, Switzerland), Richard S. Lewis (Stanford University, USA), Liangyi Chen (Beijing University, China), and Cristina Ulivieri,

bioRxiv preprint doi: https://doi.org/10.1101/663088; this version posted June 6, 2019. The copyright holder for this preprint (which was not certified by peer review) is the author/funder, who has granted bioRxiv a license to display the preprint in perpetuity. It is made available under aCC-BY 4.0 International license.

(Universita degli studi di Siena, Italy), respectively. The STIM1 (c.251A>G; p.D84G, c.910C>T; p.R304W) and ORAI1 (c.319G>A; p.V107M) point mutations were introduced by site-directed mutagenesis using the Pfu DNA polymerase (Stratagene, La Jolla, USA).

Cell culture

C2C12 murine myoblasts were cultured in DMEM, supplemented with 20% fetal calf serum (FCS) and 0.5% gentamycin (all Gibco Life Technologies, Carlsbad, USA), grown at 37°C and 5% CO_2, and transfected using Lipofectamine® 2000 (Invitrogen Life Technologies Carlsbad, USA) at 50% confluency in Opti-MEM (Gibco Life Technologies). HeLa cells were grown in DMEM with 5% FCS and 0.5% gentamycin and transfected at 70% confluency using Lipofectamine® 2000. Co-expression experiments were conducted using a 1:1 plasmid ratio.

Twenty-four hours post transfection, cells seeded on glass slides were fixed using 4% paraformaldehyde (PFA) for 20 min at RT, treated with 50mM ammonium chloride (NH4Cl) for 15 min and rinsed in 1xPBS. Nuclei were stained with DAPI (Sigma Aldrich), and the coverslips were mounted using FluorSave reagent (Calbiochem, Darmstadt, Germany). Cells were classified according to the cytosolic or nuclear localization of the eGFP-NFAT signal, and the statistical significance was assessed through one-way ANOVA followed by Dunnett's post-hoc test. All experiments were performed in triplicate and monitored with the Leica TCS SP8 AOBS inverted confocal microscope equipped with a Leica HCX PL APO CS2 63x/1.4 oil immersion objective (Leica, Wetzlar, Germany).

Total Internal Reflection Fluorescence (TIRF) microscropy

The TIRF plane of acquisition was determined according to the YFP fluorescence detected at the plasma membrane, and the images were acquired at resting state and following addition of 2µM thapsigargin (Sigma-Aldrich, Saint Louis, USA) using a Nikon TI-eclipse inverted microscope equipped with a 100x, 1.49 NA oil-immersion objective (Nikon, Tokyo, Japan).

bioRxiv preprint doi: https://doi.org/10.1101/663088; this version posted June 6, 2019. The copyright holder for this preprint (which was not certified by peer review) is the author/funder, who has granted bioRxiv a license to display the preprint in perpetuity. It is made available under aCC-BY 4.0 International license.

Correlative Light and Electron Microscopy (CLEM)

Cells were cultured on micro-patterned aclar supports (29), transfected with WT or mutant YFP-STIM1. Cells were precisely located and imaged by confocal microscopy (Leica TCS SP2-AOBS), and then chemically fixed with 0.1M sodium cacodylate buffer containing 2.5% paraformaldehyde and 2.5% glutaraldehyde, and post-fixed in 1% osmium tetroxide for 1h at 4°C. After extensive washing in distilled water, cells were incubated in 1% uranyl acetate for 1h at 4°C, dehydrated through a graded series of ethanol solutions, and embedded in epoxy resin polymerized 48h at 60°C. Ultrathin sections (60 nm) were mounted on pioloform-coated slot grids and examined with a Philips CM12 (80 kV) electron microscope equipped with a Gatan ORIUS 1000 CCD camera (FEI Company Hillsboro, USA).

RESULTS

TAM and STRMK mutants constitutively cluster at the plasma membrane

We first assessed the effect of the TAM and STRMK-related *STIM1* mutations on the SOCE-dependent accumulation of STIM1 in vicinity to the plasma membrane. To this aim, we transfected C2C12 myoblasts with WT or mutant (TAM D84G or STRMK R304W) YFP-STIM1, and monitored the fluorescence by TIRF microscopy. Cells expressing WT STIM1 showed a diffuse signal inside the cell at the resting state, and addition of 2 µM thapsigargin induced Ca^{2+}-store depletion and the formation of STIM1 clusters at the plasma membrane (Figure 1a). This is in agreement with previous studies showing that STIM1 migrates to the plasma membrane and clusters upon SOCE activation (30). In contrast, cells transfected with STIM1 D84G or R304W displayed clusters at the plasma membrane independently of thapsigargin treatment. This supports the idea that both TAM and STRMK-related *STIM1* mutations involve a gain-of-function resulting in constitutive STIM1 clustering despite replete Ca^{2+} stores.

bioRxiv preprint doi: https://doi.org/10.1101/663088; this version posted June 6, 2019. The copyright holder for this preprint (which was not certified by peer review) is the author/funder, who has granted bioRxiv a license to display the preprint in perpetuity. It is made available under aCC-BY 4.0 International license.

Figure 1: **Impact of TAM and STRMK mutations on STIM1 clustering.** (a) TIRF microscopy on transfected C2C12 muscle cells demonstrates that wild type STIM1 has a diffuse localization inside the cell, and clusters at the vicinity of the plasma membrane upon Ca^{2+} store depletion through thapsigargin (TG). In contrast, both TAM D84G and STRMK R304W mutants cluster without TG treatment and independently of the reticular Ca^{2+} load. (b) Co-transfection of C2C12 cells with differentially tagged STIM1 constructs shows that D84G and R304W STIM1 sequester wild type STIM1 to the clusters, revealing a dominant effect.

TAM and STRMK mutants sequester WT STIM1

Both TAM and Stormorken syndrome result from heterozygous *STIM1* missense mutations (4, 10-12). To investigate a potential effect of mutant STIM1 on the wild type protein, we co-transfected C2C12 cells with WT or mutant YFP-STIM1 and WT mCherry-STIM1. Cells co-expressing differently tagged WT proteins displayed diffuse overlapping signals. Addition of thapsigargin provoked co-clustering of both WT proteins, illustrating that the fluorescent YPF and mCherry tags do not impact on the intracellular localization or clustering of STIM1 (Figure 1b). Cells co-expressing D84G or R304W with WT STIM1 exhibited major STIM1 clusters of overlapping YFP and mCherry signals without thapsigargin treatment. These results demonstrate that both TAM and STRMK mutants recruit wild type STIM1 to the clusters without Ca^{2+} store depletion, and thereby evidence a dominant effect leading to the constitutive clustering of WT STIM1.

TAM and STRMK mutants recruit ORAI1 and are less sensitive to Ca^{2+} influx

The cytosolic coiled-coil domains of STIM1 contain the STIM1-ORAI1 activating domain (SOAR), which is essential for the interaction with the plasma membrane Ca^{2+} channel ORAI1 (26, 31, 32). To examine the effect of the TAM and STRMK mutations on the recruitment of ORAI1 to the STIM1 clusters, we transfected C2C12 cells with WT or mutant mCherry-STIM1

bioRxiv preprint doi: https://doi.org/10.1101/663088; this version posted June 6, 2019. The copyright holder for this preprint (which was not certified by peer review) is the author/funder, who has granted bioRxiv a license to display the preprint in perpetuity. It is made available under aCC-BY 4.0 International license.

and WT ORAI1-eGFP (Figure 2). When co-expressed, WT STIM1 and WT ORAI1 significantly co-cluster, and we also observed clusters containing STIM1 and ORAI1 in cells expressing mutant D84G or R304W STIM1 and WT ORAI1. To investigate the influence of Ca^{2+} entry on the recruitment of ORAI1 to the STIM1 clusters, we next co-transfected HeLa cells with WT or mutant mCherry-STIM and mutant V107M ORAI1-eGFP (Figure 2). The V107M mutation affects an essential amino acid of the pore-forming unit of ORAI1, and has been shown to generate a channel with constant Ca^{2+} permeability (15, 33). Major clusters were found in more than 80% of the cells expressing mutant STIM1 and mutant ORAI1, demonstrating that the leaky V107M ORAI1 channel is largely recruited to the D84G or R304W STIM1 clusters. In contrast, less than 10% of the cells expressing wild type STIM1 and mutant ORAI1 displayed prominent clusters. These data illustrate that steady Ca^{2+} inflow through V107M ORAI1 efficiently disassembles or prevents the formation of wild type STIM1 clusters and thereby inactivates SOCE, while the mutation-induced STIM1 clusters persist independently of the Ca^{2+} flux through the CRAC channel.

Figure 2: **Impact of the TAM and STRMK mutations on ORAI1 recruitment.** Confocal microscopy on co-transfected C2C12 cells shows that wild-type STIM1 co-localizes with wild-type ORAI1 in the clusters, but no clusters are seen in cells expressing wild-type STIM1 and the leaky V107M ORAI1 channel. In contrast, both STIM1 mutants D84G and R304W co-localize with V107M ORAI1 in clusters. For quantification, between 100 and 200 cells were counted per experiment and per condition. The total number of counted cells was set to 100%, the percentage of cells with major STIM1/ORAI1 clusters corresponds to the yellow bar, cells with minor cluster to the blue bar, and cells without clusters to the green bar. Error bars represent the standard deviation (SD), and the statistical difference compared to the first column of the set is indicated by * for cells without clusters and by # for cells with major clusters. P-value < 0.001:*** or ###.

bioRxiv preprint doi: https://doi.org/10.1101/663088; this version posted June 6, 2019. The copyright holder for this preprint (which was not certified by peer review) is the author/funder, who has granted bioRxiv a license to display the preprint in perpetuity. It is made available under aCC-BY 4.0 International license.

TAM and STRMK mutants increase nuclear NFAT translocation

NFATc2 (nuclear factor of activated T cells) belongs to the NFAT family of transcription factors. It has a cytosolic localization when inactive, and gets dephosphorylated through calcineurin upon increased cytosolic Ca^{2+} levels, resulting in nuclear import (34). The ratio of nuclear versus cytoplasmic NFAT therefore reflects the Ca^{2+} concentration in the cytosol and represents a suitable parameter to assess the downstream effect of excessive Ca^{2+} entry resulting from *STIM1* mutations. In accordance, previous studies have shown that constitutively active STIM1 induces major NFAT translocation to the nucleus (35). To assess if the *STIM1* TAM and STRMK mutations similarly promote nuclear NFAT import, we co-transfected WT or mutant mCherry-STIM1 with eGFP-NFAT and quantified the intracellular NFAT localization (Figure 3). About 21% of the cells expressing WT STIM1 showed a nuclear NFAT localization. Following caffeine treatment, known to induce Ca^{2+} release from the reticulum to the cytosol, nuclear NFAT was observed in 73% of the cells. Cells exogenously expressing D84G or R304W STIM1 displayed major nuclear NFAT translocation in the absence of caffeine treatment, with intense nuclear GFP signals in 58% and 61% of the cells, respectively. Quantification of the NFAT signal in the cytoplasm versus the nucleus revealed a ratio of 1.8 for cells expressing WT STIM, a ratio of 0.4 when treated with caffeine, and a ratio of 0.1 for cells expressing mutant D84G or R304W STIM1, illustrating that NFAT is mostly nuclear in cells transfected with mutant STIM1. Taken together, the STIM1 mutations D84G and R304W similarly and significantly promote nuclear NFAT import, demonstrating a downstream effect of cellular Ca^{2+} excess induced by *STIM1* mutations.

Figure 3: **Impact of the TAM and STRMK mutations on NFAT localization.** Confocal microscopy on transfected HeLa cells and quantification shows a nuclear NFAT signal in 21% and 73% of cells expressing WT STIM1 before and after caffeine treatment. In untreated cells expressing D84G or R304W STIM1, nuclear NFAT was seen in 58% and 61% of the cells,

bioRxiv preprint doi: https://doi.org/10.1101/663088; this version posted June 6, 2019. The copyright holder for this preprint (which was not certified by peer review) is the author/funder, who has granted bioRxiv a license to display the preprint in perpetuity. It is made available under aCC-BY 4.0 International license.

respectively. For quantification, between 100 and 200 cells per condition were counted in three independent experiments. The total number of counted cells was set to 100%, and the bars show the percentage of cells with nuclear NFAT in yellow and the percentage of cells with cytosolic NFAT in orange. Error bars represent the standard deviation. The statistical differences compared to cells transfected with WT STIM1 are indicated by * for nuclear NFAT and # for cytoplasmic NFAT. P-value < 0.001:*** or ###.

TAM and STRMK mutants promote circular membrane stack formation

Tubular aggregates are regular arrays of single- or double-walled membrane tubules appearing as honeycomb-like structures on transverse muscle sections, and are the histopathological hallmark of TAM and Stormoken syndrome (1, 2, 20, 36). To investigate the tubular aggregate formation *in cellulo*, we performed correlated light and electron microcopy (CLEM) on HeLa cells transfected with WT or mutant YFP-STIM1 constructs. We observed membrane stacks in cells exogenously expressing D84G or R304W STIM1, but not in cells transfected with wild-type STIM1 (Figure 4). These membrane stacks were most often found with a circular shape and connected with the endoplasmic reticulum. Our observations illustrate that STIM1 harboring amino acid substitutions found in TAM and Stormorken syndrome patients induce the emergence of aberrant membrane accumulations, potentially representing the first step of tubular aggregate formation.

Figure 4: **Impact of the TAM and STRMK mutations on membrane architecture.** CLEM allows the analysis of the same cell by light and electron microscopy. In areas corresponding to fluorescent STIM1 cluster, we observed circular membrane stacks in HeLa cells exogenously expressing the STIM1 mutants D84G or R304W, but not in cells transfected with WT STIM1.

DISCUSSION

bioRxiv preprint doi: https://doi.org/10.1101/663088; this version posted June 6, 2019. The copyright holder for this preprint (which was not certified by peer review) is the author/funder, who has granted bioRxiv a license to display the preprint in perpetuity. It is made available under aCC-BY 4.0 International license.

In this study, we investigated the molecular impact of *STIM1* mutations associated with tubular aggregate myopathy (TAM) and Stormorken syndrome (STRMK) at different levels of the SOCE pathway. We and others have previously shown that the TAM and STRMK mutations induce constitutive STIM1 clustering and activation of the Ca^{2+} entry channels (4, 10-12). Here we addressed and compared the sequence of events leading to the cellular defects of TAM and Stormorken syndrome, and we found that the TAM D84G and STRMK R304W mutants similarly impact on STIM1 clustering, ORAI1 recruitment, Ca^{2+}-dependent nuclear translocation of NFAT, and the formation of circular membrane stacks.

The STIM1 mutations have multiple effects on cluster formation

Through TIRF experiments we showed that both TAM D84G and STRMK R304W STIM1 mutants constitutively cluster in the vicinity of the plasma membrane and recruit ORAI1 to the clusters although the amino acid substitutions affect different STIM1 protein domains. The EF-hand D84G mutation is believed to directly or indirectly impair Ca^{2+} sensing, resulting in STIM1 unfolding, clustering, and exposure of the SOAR domain mediating the interaction with ORAI1 (1, 3). The luminal R304W mutation does not interfere with Ca^{2+} binding. Instead, a recent study revealed that it induces a helical elongation within the coiled-coil domain, and thereby promotes STIM1 clustering and the exposure of the SOAR domain (37). In both cases, the mutations induce constitutive ORAI1 binding and activation, resulting in major extracellular Ca^{2+} influx despite replete Ca^{2+} stores (4, 10-12).

In agreement with previous studies (26), we observed that exogenously expressed wild-type STIM1 and ORAI1 co-localize and cluster in cells. However, co-expression of wild-type STIM1 and V107M ORAI1, previously described to generate a leaky channel with reduced Ca^{2+} selectivity (15, 33), leads to a diffuse reticular distribution of STIM1. We therefore conclude that the constant ion entry through the permeable ORAI1 V107M channel either

bioRxiv preprint doi: https://doi.org/10.1101/663088; this version posted June 6, 2019. The copyright holder for this preprint (which was not certified by peer review) is the author/funder, who has granted bioRxiv a license to display the preprint in perpetuity. It is made available under aCC-BY 4.0 International license.

dissipates the STIM1 clusters or prevents their formation. It is known that massive Ca^{2+} entry generates hyperpolarized potentials at the intracellular channel gate, and thereby promotes a rapid inactivation of ORAI1 and the dissociation of STIM1 from ORAI1 (Ca^{2+}-dependent inactivation, CDI)(38, 39). In contrast to wild-type STIM1, both TAM and STRMK mutants efficiently recruited V107M ORAI1 to the clusters. This suggests that the interaction between the STIM1 mutants and the leaky ORAI1 channel is insensitive to elevated local Ca^{2+} levels, and that the consequential reduction of CDI significantly contributes to excessive extracellular Ca^{2+} entry. Consistently, decreased CDI was measured in lymphoblasts from a Stormorken syndrome patient, resulting in elevated basal Ca^{2+} levels (12).

We furthermore found that the clusters in cells co-expressing wild-type and mutant STIM1 are formed by both proteins despite replete Ca^{2+} stores. This indicates that the TAM or STRMK mutants are able to oligomerize with wild type STIM1 and to sequester the non-mutated protein to the clusters. Such an effect has not yet been described for *STIM1* mutations, and demonstrates that wild-type STIM1 contributes to the constitutive activation of ORAI1 and the excessive extracellular Ca^{2+} entry characterizing TAM and Stormorken syndrome.

The downstream effects of excessive Ca^{2+} entry

As a consequence of constitutive STIM1 and ORAI1 activation, myoblasts from TAM/STRMK patients were found to exhibit increased basal Ca^{2+} levels in the cytosol (4, 5, 7, 10-12). Ca^{2+} is a physiological key factor triggering numerous signalling cascades including the NFAT pathway. The NFAT transcription factors mainly reside in the cytosol at low Ca^{2+} concentrations, and become phosphorylated upon rising Ca^{2+} levels and translocate to the nuclei (34). In agreement, we found that cells expressing mutant STIM1 and manifesting prominent STIM1/ORAI1 clusters also displayed major nuclear NFAT translocation as compared to cells expressing wild- type STIM1. This is consistent with previous reports showing that the

bioRxiv preprint doi: https://doi.org/10.1101/663088; this version posted June 6, 2019. The copyright holder for this preprint (which was not certified by peer review) is the author/funder, who has granted bioRxiv a license to display the preprint in perpetuity. It is made available under aCC-BY 4.0 International license.

exogenous expression of constitutively active STIM1 causes nuclear NFAT import (35), while silencing of STIM1 prevents NFAT translocation (40). In this context it is interesting to note that *STIM1* belongs to the NFAT target genes (41), suggesting a positive feedback controlling SOCE that might modulate the disease development of TAM and Stormorken syndrome.

Tubular aggregates are the histopathological hallmark in skeletal muscle of patients with tubular aggregate myopathy and Stormorken syndrome (20, 42, 43). Although it is not fully understood how the tubular aggregates form, they were shown to contain sarcoplasmic reticulum proteins and large amounts of Ca^{2+} (19), and are therefore likely to be the consequence of excessive Ca^{2+} storage in the reticulum. Accordingly, constitutive SOCE activation was shown to induce the formation of membrane stacks in transfected cells (44), and our CLEM experiments on cells expressing mutant STIM1 identified multilayer reticulum membranes of circular shape, which may represent the first step of tubular aggregate formation. Of note, tubular aggregates were not seen in the TAM/STRMK mouse model harbouring the STIM1 R304W mutation and clinically recapitulating the human disorder (45), demonstrating that tubular aggregate formation is species-specific and rather a consequence than a cause of the disease.

Common pathomechanisms in tubular aggregate myopathy and Stormorken syndrome

Tubular aggregate myopathy essentially affects skeletal muscle, and a subset of TAM patients harboring STIM1 EF-hand mutations additionally manifested one or several signs of Stormorken syndrome (3-5, 8, 9, 18). Conversely, Stormorken syndrome patients carrying the most common R304W mutation usually present the full clinical picture of TAM, miosis, thrombocytopenia, hyposplenism, ichthyosis, short stature, and dyslexia (7, 10-14), but individual patients with muscle weakness as the main clinical sign were also reported (9). This illustrates that TAM and Stormorken syndrome form a clinical continuum, and raises the question on the underlying common and diverging pathomechanisms. Here we investigated and

bioRxiv preprint doi: https://doi.org/10.1101/663088; this version posted June 6, 2019. The copyright holder for this preprint (which was not certified by peer review) is the author/funder, who has granted bioRxiv a license to display the preprint in perpetuity. It is made available under aCC-BY 4.0 International license.

compared the SOCE pathway defects in cells expressing STIM1 mutants, and we uncovered that the TAM and STRMK mutants had a comparable effect on cluster formation, ORAI1 recruitment, nuclear NFAT translocation, and membrane rearrangements, indicating that TAM and Stormorken syndrome involve a common pathomechanism. The phenotypic differences between both disorders might result from a different mutational impact on fast Ca^{2+}-dependent inactivation (CDI), corresponding to the inactivation of ORAI1 through high local Ca^{2+} levels. Indeed, electrophysiological studies have shown that the R304W mutant suppresses fast CDI, while STIM1 harboring a luminal amino acid substitution was indistinguishable from the wild-type (12). This suggests that R304W, but not the EF-hand mutations causes a prolonged Ca^{2+} influx and might account for the significant aberrations in multiple tissues in patients with Stormorken syndrome. Alternatively, especially the cytosolic STIM1 R304W mutation might have an additional pathogenic effect on other interaction partners as the non-selective TRPC channels (46), and the full clinical picture of Stormorken syndrome would then result from the excessive entry of Ca^{2+} and other cations in the different tissues.

Concluding remarks

Here we demonstrate that missense mutations in different STIM1 domains have a similar pathogenic effect on SOCE and downstream pathways. Our finding that *STIM1* mutations exert a dominant effect points to a suitable therapeutic approach for TAM and Stormorken syndrome through an allele-specific downregulation of *STIM1* expression. The resulting reduction of the STIM1 protein level is thereby not expected to be pathogenic as heterozygous carriers of *STIM1* loss-of-function mutations, associated with immunodeficiency, are healthy(2).

ACKNOWLEDGEMENTS

We thank Catherine Koch and Pascal Kessler for their outstanding technical help, and Nicolas Demaurex (University of Geneva, Switzerland), Richard S. Lewis (Stanford University, USA),

bioRxiv preprint doi: https://doi.org/10.1101/663088; this version posted June 6, 2019. The copyright holder for this preprint (which was not certified by peer review) is the author/funder, who has granted bioRxiv a license to display the preprint in perpetuity. It is made available under aCC-BY 4.0 International license.

Liangyi Chen (Beijing University, China), and Cristina Ulivieri, (Universita degli studi di Siena, Italy) for providing the plasmids.

CONFLICT OF INTEREST STATEMENT

None of the authors declares a conflict of interests.

AUTHOR CONTRIBUTIONS

JL and JB designed the study and supervised the research, GAP and CS performed the experiments, GAP, CS, RSR, and JB analyzed the data, GAP, JL, and JB wrote the manuscript.

REFERENCES

1. Bohm J, Laporte J. Gain-of-function mutations in STIM1 and ORAI1 causing tubular aggregate myopathy and Stormorken syndrome. Cell Calcium. 2018;76:1-9.

2. Lacruz RS, Feske S. Diseases caused by mutations in ORAI1 and STIM1. Ann N Y Acad Sci. 2015;1356:45-79.

3. Bohm J, Chevessier F, Koch C, Peche GA, Mora M, Morandi L, et al. Clinical, histological and genetic characterisation of patients with tubular aggregate myopathy caused by mutations in STIM1. J Med Genet. 2014;51(12):824-33.

4. Bohm J, Chevessier F, Maues De Paula A, Koch C, Attarian S, Feger C, et al. Constitutive activation of the calcium sensor STIM1 causes tubular-aggregate myopathy. Am J Hum Genet. 2013;92(2):271-8.

5. Walter MC, Rossius M, Zitzelsberger M, Vorgerd M, Muller-Felber W, Ertl-Wagner B, et al. 50 years to diagnosis: Autosomal dominant tubular aggregate myopathy caused by a novel STIM1 mutation. Neuromuscul Disord. 2015;25(7):577-84.

bioRxiv preprint doi: https://doi.org/10.1101/663088; this version posted June 6, 2019. The copyright holder for this preprint (which was not certified by peer review) is the author/funder, who has granted bioRxiv a license to display the preprint in perpetuity. It is made available under aCC-BY 4.0 International license.

353 6. Hedberg C, Niceta M, Fattori F, Lindvall B, Ciolfi A, D'Amico A, et al. Childhood onset
354 tubular aggregate myopathy associated with de novo STIM1 mutations. J Neurol.
355 2014;261(5):870-6.
356 7. Harris E, Burki U, Marini-Bettolo C, Neri M, Scotton C, Hudson J, et al. Complex
357 phenotypes associated with STIM1 mutations in both coiled coil and EF-hand domains.
358 Neuromuscul Disord. 2017;27(9):861-72.
359 8. Noury JB, Bohm J, Peche GA, Guyant-Marechal L, Bedat-Millet AL, Chiche L, et al.
360 Tubular aggregate myopathy with features of Stormorken disease due to a new STIM1
361 mutation. Neuromuscul Disord. 2017;27(1):78-82.
362 9. Markello T, Chen D, Kwan JY, Horkayne-Szakaly I, Morrison A, Simakova O, et al.
363 York platelet syndrome is a CRAC channelopathy due to gain-of-function mutations in STIM1.
364 Mol Genet Metab. 2015;114(3):474-82.
365 10. Misceo D, Holmgren A, Louch WE, Holme PA, Mizobuchi M, Morales RJ, et al. A
366 dominant STIM1 mutation causes Stormorken syndrome. Hum Mutat. 2014;35(5):556-64.
367 11. Morin G, Bruechle NO, Singh AR, Knopp C, Jedraszak G, Elbracht M, et al. Gain-of-
368 Function Mutation in STIM1 (P.R304W) Is Associated with Stormorken Syndrome. Hum
369 Mutat. 2014;35(10):1221-32.
370 12. Nesin V, Wiley G, Kousi M, Ong EC, Lehmann T, Nicholl DJ, et al. Activating
371 mutations in STIM1 and ORAI1 cause overlapping syndromes of tubular myopathy and
372 congenital miosis. Proc Natl Acad Sci U S A. 2014;111(11):4197-202.
373 13. Alonso-Jimenez A, Ramon C, Dols-Icardo O, Roig C, Gallardo E, Clarimon J, et al.
374 Corpus callosum agenesis, myopathy and pinpoint pupils: consider Stormorken syndrome. Eur
375 J Neurol. 2018;25(2):e25-e6.

bioRxiv preprint doi: https://doi.org/10.1101/663088; this version posted June 6, 2019. The copyright holder for this preprint (which was not certified by peer review) is the author/funder, who has granted bioRxiv a license to display the preprint in perpetuity. It is made available under aCC-BY 4.0 International license.

14. Borsani O, Piga D, Costa S, Govoni A, Magri F, Artoni A, et al. Stormorken Syndrome Caused by a p.R304W STIM1 Mutation: The First Italian Patient and a Review of the Literature. Front Neurol. 2018;9:859.

15. Bohm J, Bulla M, Urquhart JE, Malfatti E, Williams SG, O'Sullivan J, et al. ORAI1 Mutations with Distinct Channel Gating Defects in Tubular Aggregate Myopathy. Hum Mutat. 2017;38(4):426-38.

16. Endo Y, Noguchi S, Hara Y, Hayashi YK, Motomura K, Miyatake S, et al. Dominant mutations in ORAI1 cause tubular aggregate myopathy with hypocalcemia via constitutive activation of store-operated Ca(2)(+) channels. Hum Mol Genet. 2015;24(3):637-48.

17. Garibaldi M, Fattori F, Riva B, Labasse C, Brochier G, Ottaviani P, et al. A novel gain-of-function mutation in ORAI1 causes late-onset tubular aggregate myopathy and congenital miosis. Clin Genet. 2017;91(5):780-6.

18. Li A, Kang X, Edelman F, Waclawik AJ. Stormorken Syndrome: A Rare Cause of Myopathy With Tubular Aggregates and Dystrophic Features. J Child Neurol. 2019;34(6):321-4.

19. Chevessier F, Marty I, Paturneau-Jouas M, Hantai D, Verdiere-Sahuque M. Tubular aggregates are from whole sarcoplasmic reticulum origin: alterations in calcium binding protein expression in mouse skeletal muscle during aging. Neuromuscul Disord. 2004;14(3):208-16.

20. Chevessier F, Bauche-Godard S, Leroy JP, Koenig J, Paturneau-Jouas M, Eymard B, et al. The origin of tubular aggregates in human myopathies. J Pathol. 2005;207(3):313-23.

21. Morgan-Hughes JA. Tubular aggregates in skeletal muscle: their functional significance and mechanisms of pathogenesis. Curr Opin Neurol. 1998;11(5):439-42.

22. Belaya K, Finlayson S, Slater CR, Cossins J, Liu WW, Maxwell S, et al. Mutations in DPAGT1 cause a limb-girdle congenital myasthenic syndrome with tubular aggregates. Am J Hum Genet. 2012;91(1):193-201.

bioRxiv preprint doi: https://doi.org/10.1101/663088; this version posted June 6, 2019. The copyright holder for this preprint (which was not certified by peer review) is the author/funder, who has granted bioRxiv a license to display the preprint in perpetuity. It is made available under aCC-BY 4.0 International license.

401 23. Guergueltcheva V, Muller JS, Dusl M, Senderek J, Oldfors A, Lindbergh C, et al.
402 Congenital myasthenic syndrome with tubular aggregates caused by GFPT1 mutations. J
403 Neurol. 2012;259(5):838-50.
404 24. Engel WK, Bishop DW, Cunningham GG. Tubular aggregates in type II muscle fibers:
405 ultrastructural and histochemical correlation. J Ultrastruct Res. 1970;31(5-6):507-25.
406 25. Boncompagni S, Protasi F, Franzini-Armstrong C. Sequential stages in the age-
407 dependent gradual formation and accumulation of tubular aggregates in fast twitch muscle
408 fibers: SERCA and calsequestrin involvement. Age (Dordr). 2012;34(1):27-41.
409 26. Park CY, Hoover PJ, Mullins FM, Bachhawat P, Covington ED, Raunser S, et al. STIM1
410 clusters and activates CRAC channels via direct binding of a cytosolic domain to Orai1. Cell.
411 2009;136(5):876-90.
412 27. Luik RM, Wu MM, Buchanan J, Lewis RS. The elementary unit of store-operated Ca2+
413 entry: local activation of CRAC channels by STIM1 at ER-plasma membrane junctions. J Cell
414 Biol. 2006;174(6):815-25.
415 28. Stathopulos PB, Zheng L, Li GY, Plevin MJ, Ikura M. Structural and mechanistic
416 insights into STIM1-mediated initiation of store-operated calcium entry. Cell.
417 2008;135(1):110-22.
418 29. Spiegelhalter C, Tosch V, Hentsch D, Koch M, Kessler P, Schwab Y, et al. From
419 dynamic live cell imaging to 3D ultrastructure: novel integrated methods for high pressure
420 freezing and correlative light-electron microscopy. PLoS One. 2010;5(2):e9014.
421 30. Liou J, Kim ML, Heo WD, Jones JT, Myers JW, Ferrell JE, Jr., et al. STIM is a Ca2+
422 sensor essential for Ca2+-store-depletion-triggered Ca2+ influx. Curr Biol. 2005;15(13):1235-
423 41.
424 31. Yuan JP, Zeng W, Dorwart MR, Choi YJ, Worley PF, Muallem S. SOAR and the
425 polybasic STIM1 domains gate and regulate Orai channels. Nat Cell Biol. 2009;11(3):337-43.

bioRxiv preprint doi: https://doi.org/10.1101/663088; this version posted June 6, 2019. The copyright holder for this preprint (which was not certified by peer review) is the author/funder, who has granted bioRxiv a license to display the preprint in perpetuity. It is made available under aCC-BY 4.0 International license.

426 32. Kawasaki T, Lange I, Feske S. A minimal regulatory domain in the C terminus of
427 STIM1 binds to and activates ORAI1 CRAC channels. Biochem Biophys Res Commun.
428 2009;385(1):49-54.
429 33. Bulla M, Gyimesi G, Kim JH, Bhardwaj R, Hediger MA, Frieden M, et al. ORAI1
430 channel gating and selectivity is differentially altered by natural mutations in the first or third
431 transmembrane domain. J Physiol. 2018.
432 34. Garcia-Cozar FJ, Okamura H, Aramburu JF, Shaw KT, Pelletier L, Showalter R, et al.
433 Two-site interaction of nuclear factor of activated T cells with activated calcineurin. J Biol
434 Chem. 1998;273(37):23877-83.
435 35. Huang GN, Zeng W, Kim JY, Yuan JP, Han L, Muallem S, et al. STIM1 carboxyl-
436 terminus activates native SOC, I(crac) and TRPC1 channels. Nat Cell Biol. 2006;8(9):1003-10.
437 36. Muller HD, Vielhaber S, Brunn A, Schroder JM. Dominantly inherited myopathy with
438 novel tubular aggregates containing 1-21 tubulofilamentous structures. Acta Neuropathol.
439 2001;102(1):27-35.
440 37. Fahrner M, Stadlbauer M, Muik M, Rathner P, Stathopulos P, Ikura M, et al. A dual
441 mechanism promotes switching of the Stormorken STIM1 R304W mutant into the activated
442 state. Nat Commun. 2018;9(1):825.
443 38. Mullins FM, Park CY, Dolmetsch RE, Lewis RS. STIM1 and calmodulin interact with
444 Orai1 to induce Ca2+-dependent inactivation of CRAC channels. Proc Natl Acad Sci U S A.
445 2009;106(36):15495-500.
446 39. Zweifach A, Lewis RS. Rapid inactivation of depletion-activated calcium current
447 (ICRAC) due to local calcium feedback. J Gen Physiol. 1995;105(2):209-26.
448 40. Aubart FC, Sassi Y, Coulombe A, Mougenot N, Vrignaud C, Leprince P, et al. RNA
449 interference targeting STIM1 suppresses vascular smooth muscle cell proliferation and
450 neointima formation in the rat. Mol Ther. 2009;17(3):455-62.

bioRxiv preprint doi: https://doi.org/10.1101/663088; this version posted June 6, 2019. The copyright holder for this preprint (which was not certified by peer review) is the author/funder, who has granted bioRxiv a license to display the preprint in perpetuity. It is made available under aCC-BY 4.0 International license.

451 41. Phuong TT, Yun YH, Kim SJ, Kang TM. Positive feedback control between STIM1 and
452 NFATc3 is required for C2C12 myoblast differentiation. Biochem Biophys Res Commun.
453 2013;430(2):722-8.
454 42. Salviati G, Pierobon-Bormioli S, Betto R, Damiani E, Angelini C, Ringel SP, et al.
455 Tubular aggregates: sarcoplasmic reticulum origin, calcium storage ability, and functional
456 implications. Muscle Nerve. 1985;8(4):299-306.
457 43. Stormorken H, Sjaastad O, Langslet A, Sulg I, Egge K, Diderichsen J. A new syndrome:
458 thrombocytopathia, muscle fatigue, asplenia, miosis, migraine, dyslexia and ichthyosis. Clin
459 Genet. 1985;28(5):367-74.
460 44. Orci L, Ravazzola M, Le Coadic M, Shen WW, Demaurex N, Cosson P. From the
461 Cover: STIM1-induced precortical and cortical subdomains of the endoplasmic reticulum. Proc
462 Natl Acad Sci U S A. 2009;106(46):19358-62.
463 45. Silva-Rojas R, Treves S, Jacobs H, Kessler P, Messaddeq N, Laporte J, et al. STIM1
464 over-activation generates a multi-systemic phenotype affecting skeletal muscle, spleen, eye,
465 skin, bones, and the immune system in mice. Hum Mol Genet. 2018.
466 46. Worley PF, Zeng W, Huang GN, Yuan JP, Kim JY, Lee MG, et al. TRPC channels as
467 STIM1-regulated store-operated channels. Cell Calcium. 2007;42(2):205-11.

Figure 2

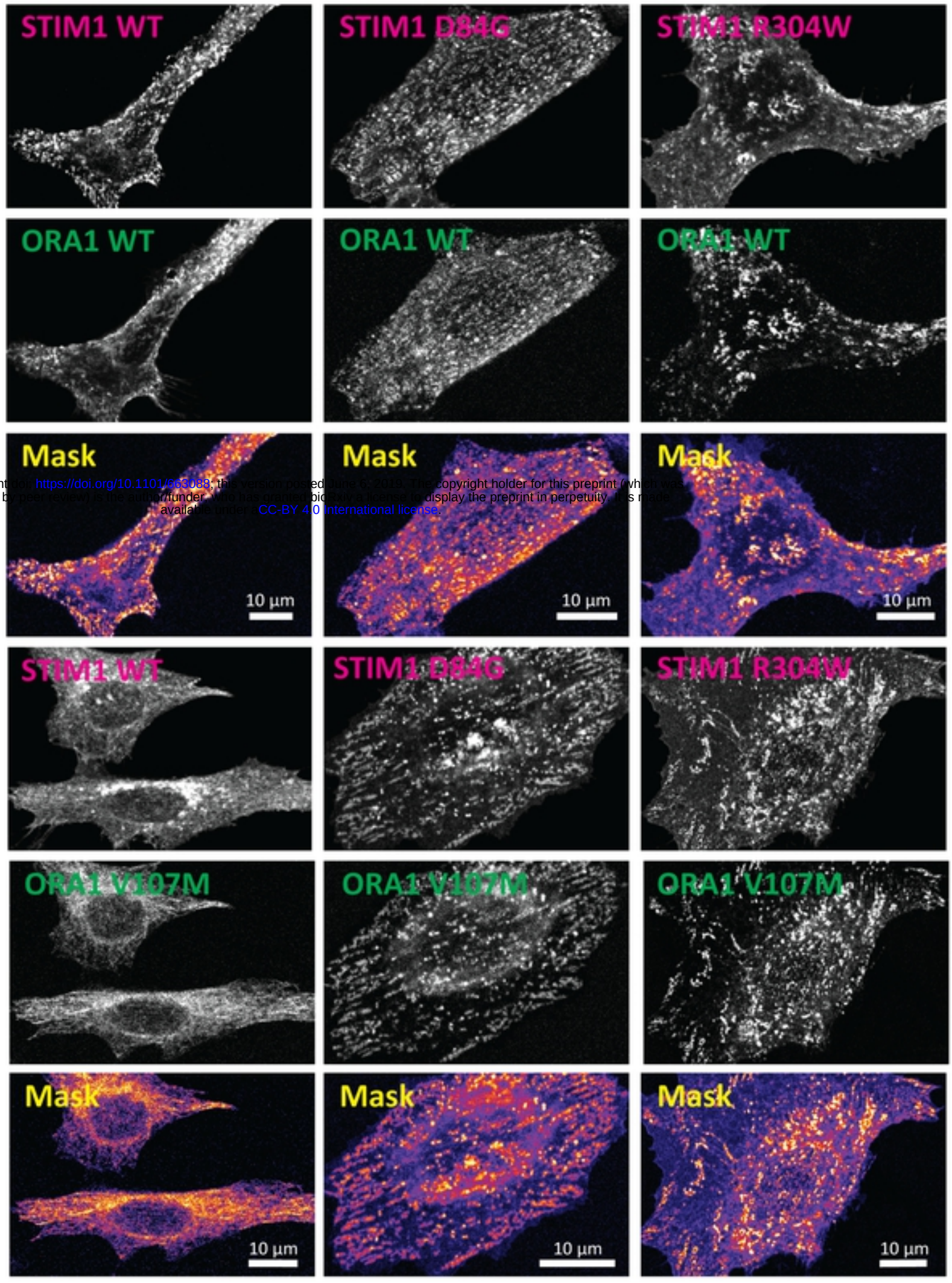

bioRxiv preprint doi: https://doi.org/10.1101/663088; this version posted June 6, 2019. The copyright holder for this preprint (which was not certified by peer review) is the author/funder, who has granted bioRxiv a license to display the preprint in perpetuity. It is made available under CC-BY 4.0 International license.

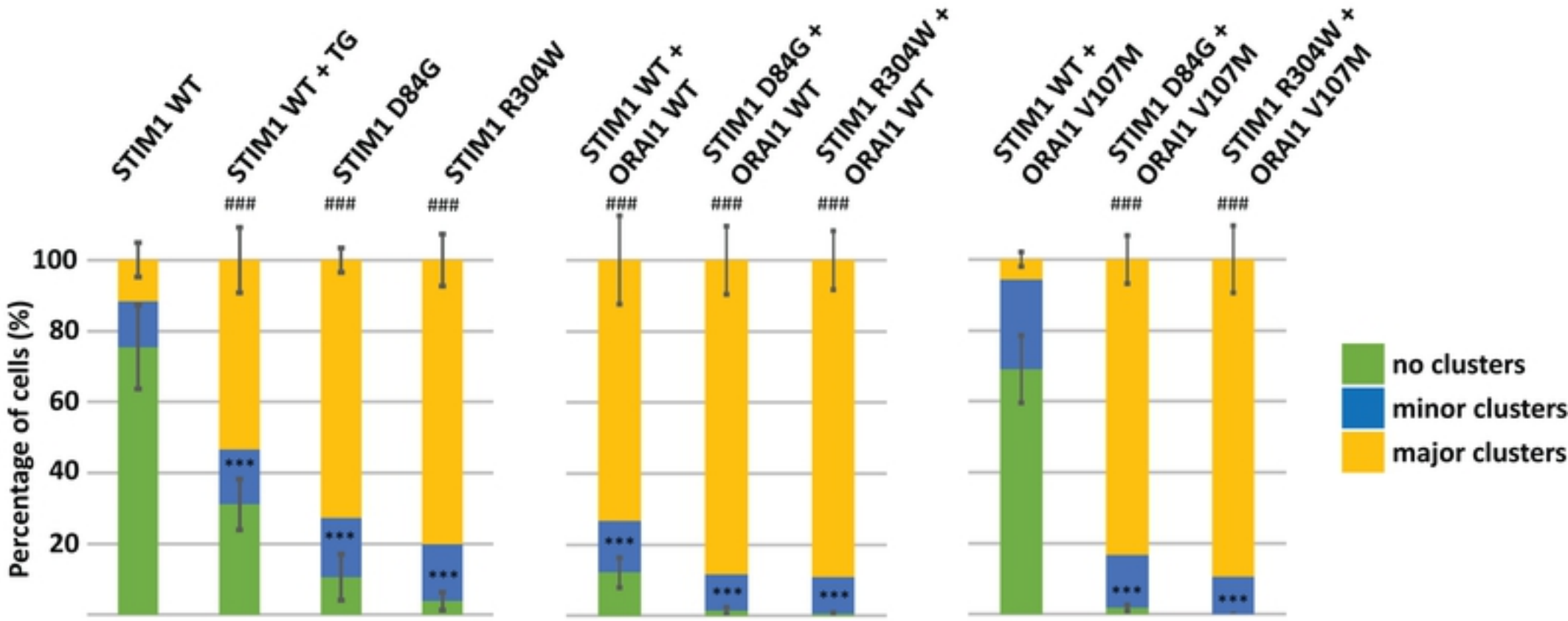

Figure 3

a

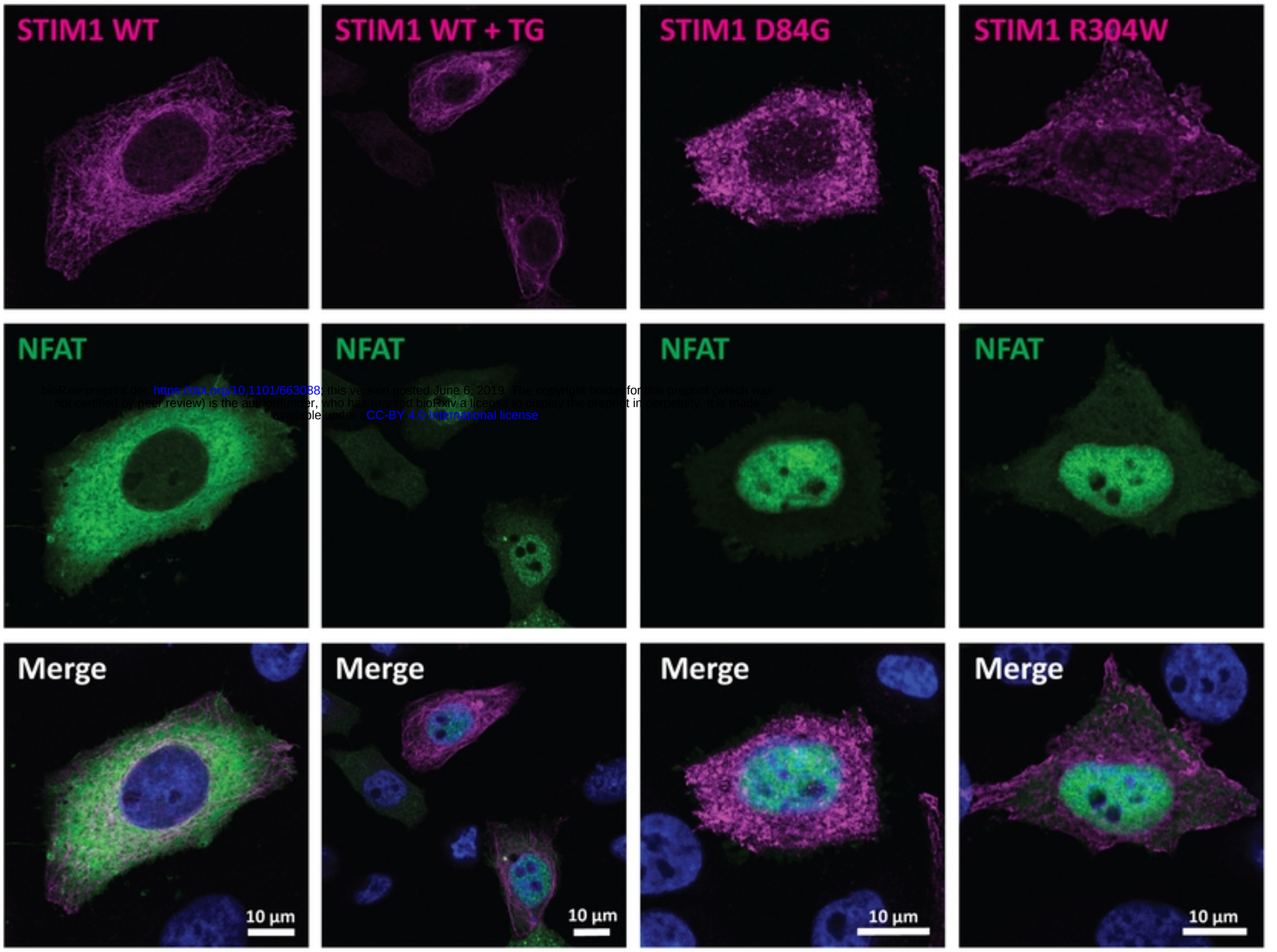

bioRxiv preprint doi: https://doi.org/10.1101/663088; this version posted June 6, 2019. The copyright holder for this preprint (which was not certified by peer review) is the author/funder, who has granted bioRxiv a license to display the preprint in perpetuity. It is made available under a CC-BY 4.0 International license

b

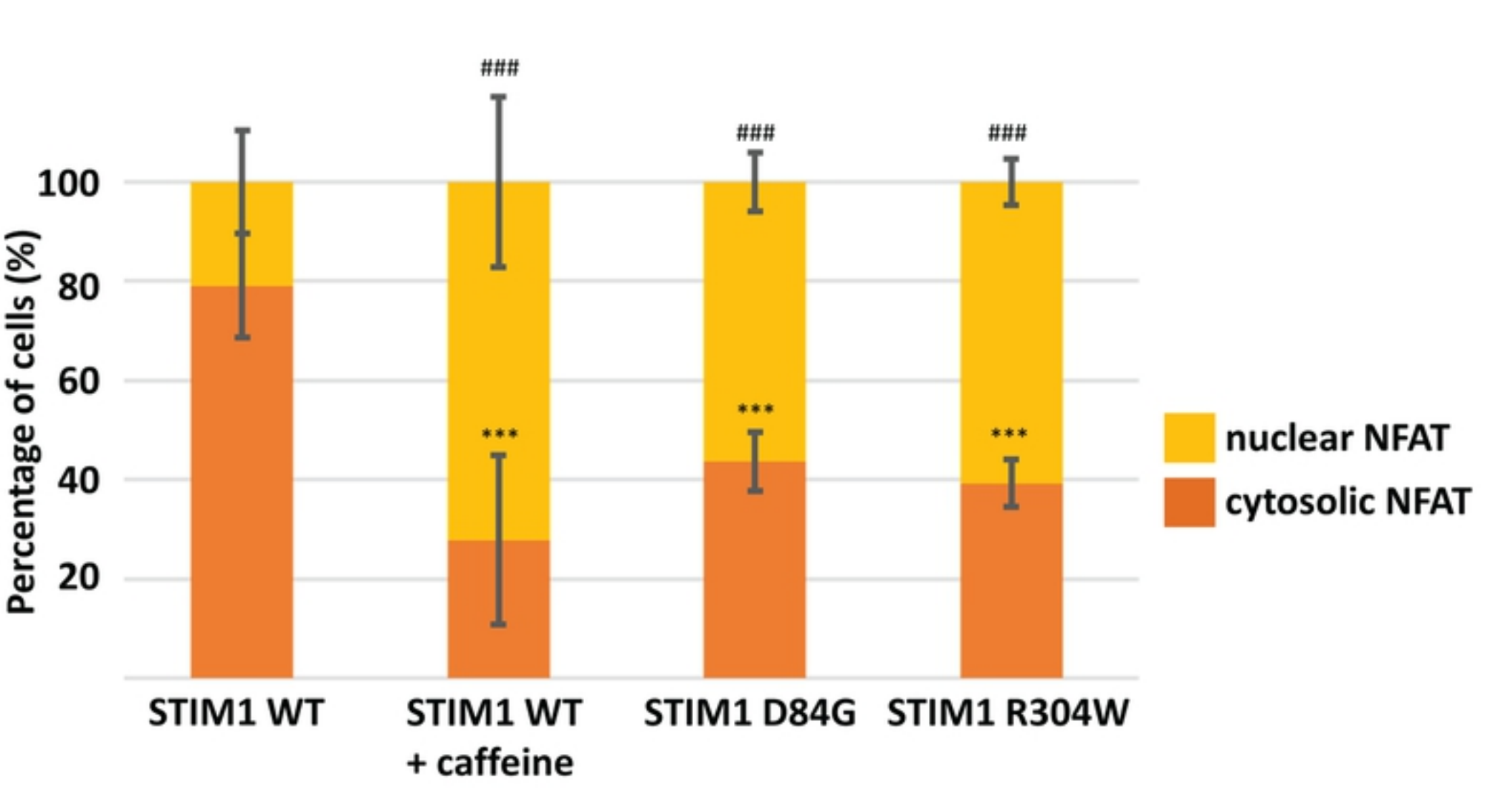

bioRxiv preprint doi: https://doi.org/10.1101/663088; this version posted June 6, 2019. The copyright holder for this preprint (which was not certified by peer review) is the author/funder, who has granted bioRxiv a license to display the preprint in perpetuity. It is made available under aCC-BY 4.0 International license.

Figure 4

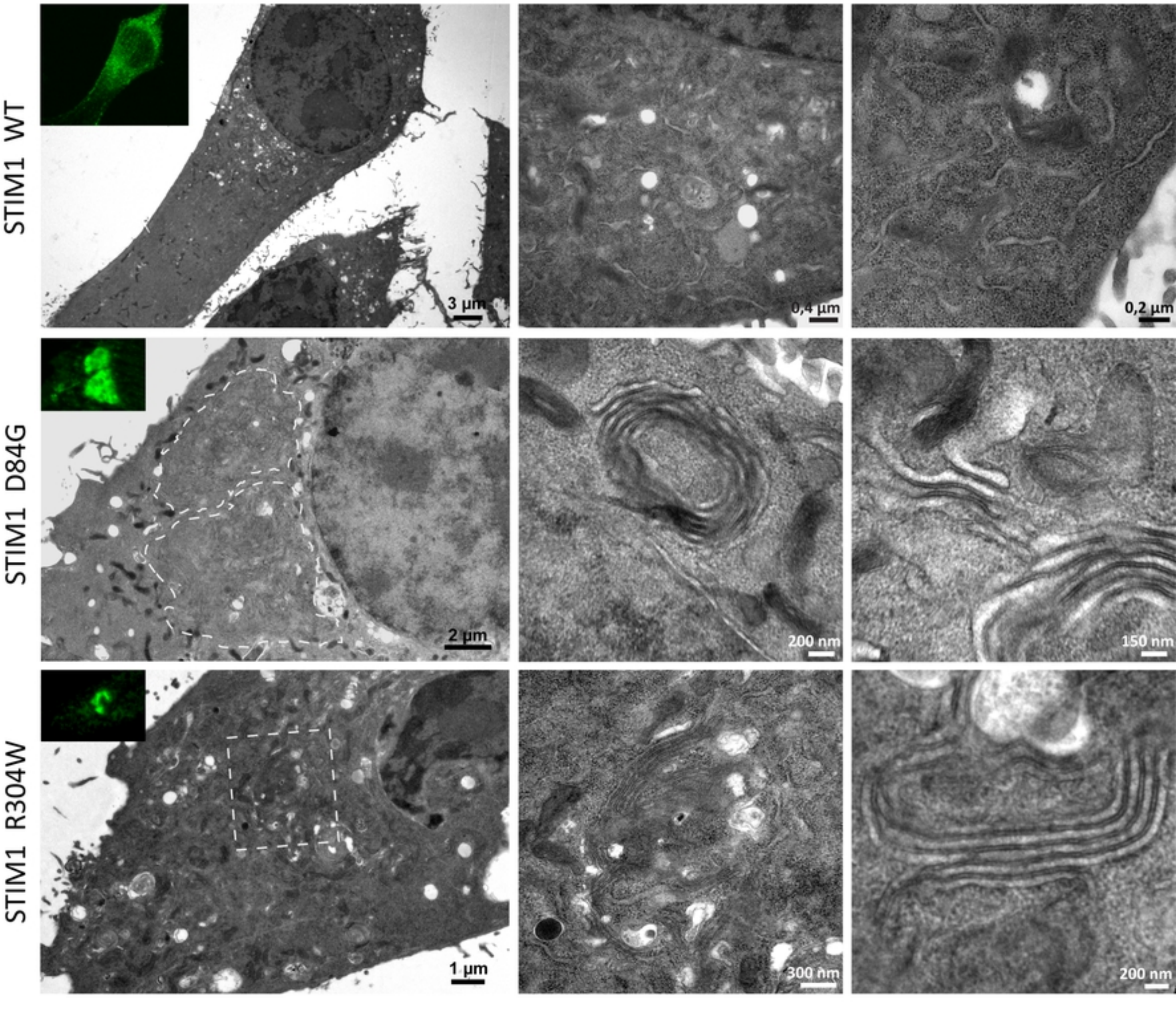

Figure 1

bioRxiv preprint doi: https://doi.org/10.1101/663088 this version posted June 6, 2019. The copyright holder for this preprint (which was not certified by peer review) is the author/funder, who has granted bioRxiv a license to display the preprint in perpetuity. It is made available under aCC-BY 4.0 International license.